Journal of Cellular Biochemistry 103:492–508 (2008)

Yeast N^{α}-Terminal Acetyltransferases Are Associated With Ribosomes

Bogdan Polevoda, Steven Brown, Thomas S. Cardillo, Sean Rigby, and Fred Sherman*

Department of Biochemistry and Biophysics, University of Rochester Medical Center, Rochester, New York 14642

Abstract N-terminal acetylation is one of the most common modifications, occurring on the vast majority of eukaryotic proteins. *Saccharomyces cerevisiae* contains three major NATs, designated NatA, NatB, and NatC, with each having catalytic subunits Ard1p, Nat3p, and Mak3p, respectively. Gautschi et al. (Gautschi et al. [2003] Mol Cell Biol 23: 7403) previously demonstrated with peptide crosslinking experiments that NatA is bound to ribosomes. In our studies, biochemical fractionation in linear sucrose density gradients revealed that all of the NATs are associated with mono- and polyribosome fractions. However only a minor portion of Nat3p colocalized with the polyribosomes. Disruption of the polyribosomes did not cause dissociation of the NATs from ribosomal subparticles. The NAT auxiliary subunits, Nat1p and Mdm20p, apparently are required for efficient binding of the corresponding catalytic subunits to the ribosomes. Deletions of the genes corresponding to auxiliary subunits significantly diminish the protein levels of the catalytic subunits, especially Nat3p, while deletions of the catalytic subunits produced less effect on the stability of Nat1p and Mdm20p. Also two ribosomal proteins, Rpl25p and Rpl35p, were identified in a TAP-affinity purified NatA sample. Moreover, Ard1p copurifies with Rpl35p-TAP. We suggest that these two ribosomal proteins, which are in close proximity to the ribosomal exit tunnel, may play a role in NatA attachment to the ribosome. J. Cell. Biochem. 103: 492–508, 2008.

Key words: N-terminal acetylation; N^{α}-terminal acetyltransferase(s); ribosome association; Rpl35p; yeast

The two cotranslational processes, cleavage of N-terminal methionine residues and N-terminal acetylation, are by far the most common modifications, occurring on the vast majority of proteins. Eukaryotic proteins initiate with methionine that is cleaved from nascent chains of most proteins by methionine aminopeptidases (MAP). Subsequently, N-terminal acetylation occurs on certain of the proteins, either containing or lacking the methionine residue. This N-terminal acetylation occurs on over one half of soluble eukaryotic proteins, but seldom on prokaryotic proteins [Jörnvall, 1975; Driessen et al., 1985; Lee et al., 1989].

N-terminal acetylation of proteins is catalyzed by N-terminal acetyltransferases (NATs) that transfer acetyl groups from acetyl-CoA to termini of α-amino groups. We have established that *Saccharomyces cerevisiae* have three major N-terminal acetyltransferases (NATs) that contain the following catalytic and auxiliary subunits:

Abbreviations used: MALDI-TOF, matrix assisted laser desorption/ionization time-of-flight MS; MAP, methionine aminopeptidase; MS, mass spectrometry; N-terminal, N^{α}-terminal; NAC, nascent polypeptide-associated complex; NAT(s), N-terminal acetyltransferase(s); Nfs^{-}, diminished or lack of growth on media containing non-fermentable carbon sources as the sole source of energy, such as glycerol or ethanol; ProA, protein A of *Staphylococcus aureus*; RP, ribosomal protein; PR, MR, and CT, the polyribosomal, monoribosomal, and cytosolic fractions, respectively; SRP, signal-recognition particle; TAP, tandem affinity purification; TEV protease, tobacco etch virus protease; t.s., temperature sensitive or sensitivity.

Grant sponsor: NIH; Grant number: R01 GM12702; Grant sponsor: National Center for Research Resources of the NIH; Grant number: RR14682.

*Correspondence to: Fred Sherman, Department of Biochemistry and Biophysics, Box 712, University of Rochester Medical Center, Rochester, NY 14642.
E-mail: Fred_Sherman@urmc.rochester.edu

Received 22 August 2006; Accepted 19 April 2007
DOI 10.1002/jcb.21418

NATs	NatA	NatB	NatC
Catalytic subunits	Ard1p	Nat3p	Mak3p
Auxiliary subunits	Nat1p	Mdm20p	Mak10p and Mak31p

Each NAT is required for acetylating different groups of proteins [Polevoda and Sherman, 2000] (Table I). Recently a new yeast NAT, Nat4p, was identified that corresponds to an acetyltransferase responsible for acetylation of the N-termini of the histones H4 and H2A [Song et al., 2003]. For consistency, we have designated the Nat4p function as NatD. In addition, another putative acetyltransferase, Nat5p [Polevoda and Sherman, 2003a], was found physically associated with NatA [Gautschi et al., 2003]. However its substrate specificity is unknown. We designated Nat5p function as NatE. It should be noted that Nat5p is not required for NatA activity [Mullen et al., 1989; Park and Szostak, 1992].

All three major NATs contain at least one auxiliary subunit in addition to a catalytic subunit [Polevoda and Sherman, 2003b] (Table I). For example, NatA contains the catalytic subunit Ard1p and the auxiliary subunit Nat1p [Mullen et al., 1989; Park and Szostak, 1992]. Both *nat1* and *ard1* mutants were unable to N-terminally acetylate in vivo the same subset of 24 normally acetylated proteins [Polevoda et al., 1999]. In addition to lacking NAT activity, both *nat1*-Δ and *ard1*-Δ mutants exhibited slower growth, derepression of the silent mating type gene *HMLα*, and failure to enter Go. Some of these phenotypes can be attributed to the lack of Sir3p and Orc1p acetylation in NatA mutants [Geissenhoner et al., 2004; Wang et al., 2004].

NatB acetyltransferase contains the catalytic subunit Nat3p [Polevoda et al., 1999] and auxiliary subunit Mdm20p [Singer et al., 2000; Polevoda et al., 2003]. The *nat3*-Δ and *mdm20*-Δ mutants exhibited the following multiple defects: slow growth; temperature, and osmotic sensitivity; deficiency in utilization of nonfermentable carbon sources (Nfs^-); reduced mating efficiency; inability to form functional actin cables; defects in mitochondrial and vacuolar inheritance; random polarity in budding; sensitivity to the antimitotic drugs; and susceptibility to the number of the DNA damaging agents [Polevoda et al., 2003]. The nat3 and mdm20 mutants have the most severe phenotypes in comparison to the *ard1* and *nat1* mutants or the *mak3*, *mak10*, and *mak31* mutants. Furthermore, a comparison of the phenotypes of NatB mutants with the phenotypes of *act1* and *tpm1* mutants altered in the N-terminal protein regions indicated that the *nat3*-Δ and *mdm20*-Δ phenotypes are due primarily to the lack of actin and tropomyosin acetylation [Singer et al., 2000; Polevoda et al., 2003] that causes the defects in transport from the mother cell to the bud of a variety of membrane-bound organelles, including mitochondria, vacuoles, Golgi elements and secretory vesicles. In addition, *nat3*-Δ and *mdm20*-Δ probably affect nuclear division and the functioning of the DNA-chromatin-containing complexes, as both mutants are sensitive to the antimitotic drugs and the DNA damaging agents [Polevoda et al., 2003].

MAK3 encodes the catalytic subunit of NatC, which is required for acetylation of the viral major coat protein, *gag*, which contains a

TABLE I. The Five Types of Yeast N-Terminal Acetyltransferases

Type	NatA	NatB	NatC	NatD	NatE
Catalytic subunit	Ard1p[a]	Nat3p[a]	Mak3p[a]	Nat4p[a]	Nat5p[a]
Auxiliary subunit	Nat1p[a,b]	Mdm20p[a]	Mak10p[a] Mak31p		Nat1p[a,b]
Substrates[c]	Ser- Ala- Gly- Thr-	Met-Glu- Met-Asp- Met-Asn- Met-Met-	Met-Ile- Met-Leu- Met-Trp- Met-Phe	Ser-Gly-Gly-Lys-etc- Ser-Gly-Arg-Gly-etc-	Unknown
No. of substrates	>2,000	>600	Low	At least 2	Unknown

[a]Subunits shown to be associated with ribosomes.
[b]We suggest that the auxiliary subunit Nat1p is common to both NatA and NatE, and that *nat1*-Δ mutants are deficient in both acetyltransferases.
[c]Acetylation occurs only on subclasses of proteins containing the indicated termini, except for Met-Glu- and Met-Asp- termini, which are apparently always acetylated.

MLRF- terminus [Tercero and Wickner, 1992; Tercero et al., 1993]. The copurification of Mak3p, Mak10p, and Mak31p suggested that these three subunits form a complex [Rigaut et al., 1999]. Moreover, protein–protein interactions between Mak3p and Mak10p, as well as between Mak31p and Mak10 were detected in two-hybrid screen [Uetz et al., 1999]. We demonstrated that each of the Mak3p, Mak10p, and Mak31p subunits are required for acetylation of the NatC-type N-terminal sequences in vivo [Polevoda and Sherman, 2001]. In addition, all three deletion strains showed similar phenotypes, including Nfs^{-} at elevated temperature [Polevoda and Sherman, 2001].

Several studies have suggested that eukaryotic MAPs and NATs are ribosome-associated. Studies in rabbit reticulocyte lysates showed that N-terminal methionine is cotranslationally removed from nascent polypeptides that are approximately 45–50 amino acids in length [Jackson and Hunter, 1970], whereas ribosomes protected the nascent polypeptides up to 30 amino acids in length from protease degradation [Rich et al., 1966; Malkin and Rich, 1967]. Vetro and Chang [2002] were the first to reported direct evidence for the association of the eukaryotic MAP with ribosomes. The yeast Map1p was primarily associated with the 60S ribosome subunit and with the 80S translational complex in the presence of magnesium (Mg^{++}). Low levels of Map1p were also detected in the 40S ribosome subunit fractions in the absence of Mg^{++}. Map1p is probably recruited from the cytosol to the 80S translational complex through an association with the 60S subunit. Also it was suggested that Map1p is localized to the 60S subunit near the exit of the polypeptide channel [Morgan et al., 2002].

Previous experiments with ovalbumin, α-crystallin, ribosomal subunit proteins and histones have shown that N-acetylation is also a cotranslational event [Pestana and Pitot, 1974; Traugh and Sharp, 1977, 1979; Tsunasawa and Sakiyama, 1984]. Kido et al. [1981] demonstrated that a transacetylase associated with the ribosome fraction from wheat germ catalyzed the transfer of acetyl groups from acetyl CoA to synthetic thymosin α_1. Results obtained in vivo and with ovalbumin mRNA translation in vitro in a reticulocyte lysate demonstrated that the initial methionine was removed, followed by the acetylation of the N-terminal glycine when the polypeptide was 41–47 residues long [Palmiter et al., 1978]. Similarly, α-crystallin was found to be cotranslationally acetylated [Strous et al., 1974], such that both secretory, ovalbumin, and nonsecretory, α-crystallin, proteins were N-terminally acetylated when a newly synthesized polypeptide has protruded from the ribosome. Also, H1 and H4 histone syntheses in an in vitro rabbit reticulocyte lysate showed that their N-terminal amino acid is Nα-acetylserine [Kecskes et al., 1976]. Evidence that human N-myristoyltransferase [Glover et al., 1997] and mammalian N-acetyltransferase [Pestana and Pitot, 1975a,b] are associated with the ribosomes also has been reported.

Moreover, Gautschi et al. [2003] revealed with peptide crosslinking experiments that NatA was quantitatively bound to ribosomes via Nat1p and that Nat1p anchored Ard1p and Nat5p to the ribosome. Nat1p also was found in close proximity to nascent polypeptides, independent of whether they were substrates for N-acetylation or not, and required longer nascent polypeptides for interaction than nascent the polypeptide-associated complex (NAC) or Ssb1p/Ssb2p complex that is involved in protein folding.

In this study, we used biochemical polyribosome fractionation to demonstrate that NatA is associated with mono- and polyribosomes and also that the other NATs, for example, NatB, NatC, and NatE, colocalized with ribosomes. The NAT noncatalytic subunits, Nat1p, and probably Mdm20p serve as anchors to the ribosome. We determined that the deletions of those auxiliary subunits, as well as *MAK10*, significantly diminished the protein levels and stability of the catalytic subunits, especially Nat3p (NatB), while deletions of the catalytic subunits Ard1p, Nat3p, and Nat5p had little effect on stability of Nat1p and Mdm20p. On the other hand, disruption of polyribosomes by removing magnesium from the buffer did not cause dissociation of the NATs from ribosomal subparticles. In addition, we biochemically purified NatA complex by TAP procedure and found several ribosomal proteins in the NatA sample, particularly Rpl25p and Rpl35p. Moreover, Ard1p copurifies with Rpl35p-TAP. We suggest that these two proteins play a role in NatA attachment to the ribosome, especially Rpl25p that recently was found to be a docking site for NAC [Wegrzyn and Deuerling, 2005; Grallath et al., 2006].

EXPERIMENTAL PROCEDURES

Yeast Strains

The strains of *S. cerevisiae* used in this study are listed in Table II. Yeast polyribosome fractionation experiments were carried out with three isogenic series, which were derived from the following parental strains: B-11679 (*MAT*α *ura3-52*); B-10190 (*MAT***a** *his3-Δ200 leu2-3,112 lys2-801 trp1-1 ura3-52*); and B-13480 (*MAT***a** *his3Δ1 leu2Δ0 met15Δ0 ura3Δ0*).

Media

Standard media, YPD and SD containing appropriate supplements have been described [Sherman, 2002]. Yeast strains were grown at 30C.

Construction of the Deletion Mutants and TAP Tagged Strains

Standard molecular biological procedures were performed as previously described [Polevoda et al., 1999]. Appropriate PCR fragments were used to disrupt genes by replacing the portions of the genes with the *URA3* or *kanMX4* genes; *MAK3*, *MAK10*, and *NAT1* were disrupted with *URA3*, whereas *ARD1*, *MAK31*, and *MDM20* were disrupted with *kanMX4* [Polevoda et al., 1999]. The corresponding primer sequences are presented in Table III. For example, for the *nat3*-Δ::*kanMX4* disruption, primers Oligo1 and Oligo2 were used to prepare the PCR fragment for transformation, and the correct disruption was identified by PCR, using the set of primers Oligo3 and Oligo4. The *mak10*-Δ::*kanMX4* and *mak31*-Δ::*kanMX4* deletants were obtained by the same procedure with the sets of primers Oligo13-Oligo16 and Oligo 17-Oligo20, respectively. Similarly, the fragment required for producing the *mdm20*-Δ::*kanMX4* disruption was prepared with Oligo5 and Oligo6 (Table III) and yeast genomic DNA made from a *mdm20*-Δ::*kanMX4* deletion strain (Invitrogen/Research Genetics, Carlsbad, CA) as a template. The plasmids pAA1131 for *mak3*-Δ::*URA3* disruptions and pAA1132 for *nat1*-Δ::*URA3* disruptions were constructed previously [Mullen et al., 1989; Tercero et al., 1993]. The *NAT3-TAP* tagged strain was described earlier [Polevoda et al., 1999]; the *ARD1-TAP* strain was obtained by similar procedure using Oligo21 and Oligo22; and the fusion gene was checked by sequencing with Oligo23. The following *MYC* tagged strains were constructed with the following pairs of

TABLE II. Yeast Strains

Strain no.	Genotype	Reference/Source
B-11679	*MAT*α ura*3-52*	Polevoda et al. [1999]
B-11706	*MAT*α *ura3-52 ard1*-Δ::*kanMX4*	Polevoda et al. [1999]
B-11815	*MAT*α *ura3-52 nat1*-Δ::*kanMX4*	Polevoda et al. [1999]
B-13924	*MAT*α *ura3-52 nat5*-Δ::*kanMX4*	This study
B-14542	*MAT*α *ura3-52 nat1*-Δ::*URA3 nat5*-Δ::*kanMX4*	This study
B-10190	*MAT***a** *his3-Δ200 leu2-3,112 lys2-801 trp1-1 ura3-52*	Polevoda et al. [1999]
B-13396	*MAT***a** *his3-Δ200 leu2-3,112 lys2-801 trp1-1 ura3-52 NAT3-TAP::TRP1*	Polevoda et al. [1999]
B-15364	*MAT***a** *his3-Δ200 leu2-3,112 lys2-801 trp1-1 ura3-52 NAT3-TAP::TRP1 mdm20-Δ::kanMX4*	This study
B-14260	*MAT***a** *his3-Δ200 leu2-3,112 lys2-801 trp1-1 ura3-52 ARD1-TAP::TRP1*	This study
B-15369	*MAT***a** *his3-Δ200 leu2-3,112 lys2-801 trp1-1 ura3-52 ARD1-TAP::TRP1 nat1-Δ::kanMX4*	This study
B-15511	*MAT***a** *his3-Δ200 leu2-3,112 lys2-801 trp1-1 ura3-52 NAT3-TAP::TRP1* p[*CEN URA3 MDM20-3×HA*]	This study
B-15332	*MAT***a** *his3Δ1 leu2Δ0 met15Δ0 ura3Δ0 NAT5-TAP::HIS3*	Open Biosystems
B-15791	*MAT***a** *his3Δ1 leu2Δ0 met15Δ0 ura3Δ0 MDM20-TAP::HIS3*	Open Biosystems
B-15349	*MAT***a** *his3Δ1 leu2Δ0 met15Δ0 ura3Δ0 MAK3-TAP::HIS3*	Open Biosystems
B-15366	*MAT***a** *his3Δ1 leu2Δ0 met15Δ0 ura3Δ0 MAK3-TAP::HIS3 mak10-Δ::kanMX4*	This study
B-15365	*MAT***a** *his3Δ1 leu2Δ0 met15Δ0 ura3Δ0 MAK3-TAP::HIS3 mak31-Δ::kanMX4*	This study
B-15431	*MAT***a** *his3Δ1 leu2Δ0 met15Δ0 ura3Δ0 MAK3-TAP::HIS3 mak10-Δ::URA3 mak31-Δ::kanMX4*	This study
B-15132	*MAT***a** *his3-Δ200 leu2-3,112 lys2-801 trp1-1 ura3-52 MAK3::3 × MYC*	This study
B-15202	*MAT***a** *his3-Δ200 leu2-3,112 lys2-801 trp1-1 ura3-52 NAT3::3 × MYC*	This study
B-15204	*MAT***a** *his3-Δ200 leu2-3,112 lys2-801 trp1-1 ura3-52 NAT5::3 × MYC*	This study
B-15303	*MAT***a** *his3-Δ200 leu2-3,112 lys2-801 trp1-1 ura3-52 MAK3::3 × MYC mak31-Δ::kanMX4*	This study
B-15306	*MAT***a** *his3-Δ200 leu2-3,112 lys2-801 trp1-1 ura3-52 MAK3::3 × MYC mak10-Δ::URA3*	This study
B-15925	*MAT***a** *his3Δ1 leu2Δ0 met15Δ0 ura3Δ0 RPL35B-TAP::HIS3*	Open Biosystems

TABLE III. Oligonucleotides Used in the Construction and Testing of the Disrupted Genes

ORF	Oligo.	Sequence (5′ → 3′)
NAT3	Oligo1	(−70) GCAAAAAACATAGCGGTGGGCGCACGTTGGTGGGCCTGG GAAGAACA GCTGAAGCTTCG
NAT3	Oligo2	(+814) TGAATAGCACAGAGGTTCATTATTATGTTCTGAGTATGA GGACGAAGGCCACTAGTGGATCTG
NAT3	Oligo3	(−142) TTCCAATGCGGTAGTGCTTAGC
NAT3	Oligo4	(+906) TATATCATTCAGTATGTACATAC
MDM20	Oligo5	(−140) CAGTCACCTTTAACGAAAATCG
MDM20	Oligo6	(+2,554) CCTCAAAAATCATATACTACTTTTTC
NAT1	Oligo7	(−40) GACAAATACCATTGAGGAAG
NAT1	Oligo8	(+2,742) GAAAAGGTCCTGGCTGTCCTGG
ARD1	Oligo9	(−42) CTAAATACATACGATCAAGCTC
ARD1	Oligo10	(+778) CTAACAGAGCTTGTGAAGAAGC
MAK3	Oligo11	(−68) GAACAAAGTTTCACAAGAGATTAC
MAK3	Oligo12	(+614) CTATATCTATACATATGATTAAAT
MAK10	Oligo13	(−51) AACTGTGCTAGTGTAGAGCAAACTTTGATAATAGCTGGTAC GTTTCCGAGAACAGCTGAAGCTTCGT
MAK10	Oligo14	(+2,255) TAGCGGGTATATAATGCTAAATATATTTTGTACAGTTAG GGTAAATTCCTGCATAGGCCACTAGT
MAK10	Oligo15	(−133) GAGATGGAGTGAAATTTCACGA
MAK10	Oligo16	(+2,318) TGGGATAATGGCATAAGGTGGC
MAK31	Oligo17	(−53) TTGATAGGGTGAAGATAGTCTTCAACAAACTTAGTAAGGG GCACAGCTGAAGCTTCGTACGC
MAK31	Oligo18	(+311) TTGCCAAGCAATTGTTACTATGGAAACTATTAGAACCATA TGCGCATAGGCCACTAGTGGATC
MAK31	Oligo19	(−100) CGCGAAGTGCATGAGTTCTGAC
MAK31	Oligo20	(+362) AGTTCAGTCCAGTTCATATTCG
ARD1	Oligo21	(+667) GATCTACTAGAGGATATCATTAAGCAAGGCGTAA ATGAT ATCATTAGAACA GCTGAAGCTTCG
ARD1	Oligo22	(+791) TGCTCAAAAAGAGCTAACAGAGCTTGT GAAGAAGCCTG GATGAAAATAGGCCACTAGTGGATCTG
ARD1	Oligo23	(+856) CCTTACTATTCATGCTCACAC
MAK3	Oligo24	(+483) AGCTGCACTCGGTCTACGTTCCTAATGCATGGCCTGGCCC GGCTGGCCACAAGGGAACAAAAGCTGG
MAK3	Oligo25	(+576) TTGTATTATTAATATATATTTTATCATCATCGAGTGTTTTT CCTTCTATAGGGCGAATTGG
MAK3	Oligo26	(+383) CTTATATGCAGGAATGGGTTT
MAK3	Oligo27	(+675) TTTTGAAACTTGATTTATTATC
NAT5	Oligo28	(+484) AATGGCGACGAACAAGATGCTATCTTATTGAAAAAACACA TTTCTAGGGAACAAAAGCTGG
NAT5	Oligo29	(+576) TACAAAGCAAAACCAAAAAAAAAAAAAAAAATTTTTCAGC CATCTGCTATAGGGCGAATTGG
NAT5	Oligo30	(+449) TGTCTATTTACCAGCAGTGGA
NAT5	Oligo31	(+676) GATGATGAATCACCAGAATAG
NAT3	Oligo32	(+541) CCGGATGGAAGAAGCCATAAATGCTATCCACATGATGTA AGATTTAGGGAACAAAAGCTGG
NAT3	Oligo33	(+633) GGTTCATTATTATGTTCTGAGTATGAGGACGAGGTAATAC ATACCCTATAGGGCGAATTGG

The position of the first nucleotide is presented, where A of the ORF ATG initiation codon is assigned position 1. The underlined sequences are homologous to the following regions: Oligo1 and 2, 13 and 14, 17 and 18, to *kanMX4* cassette; Oligo21 and 22, to template plasmid pBS1479 (pAB2629); Oligo 24, 25, 27, 28, 32, and 33, to pAB1868, respectively.

primers, using the method of Schneider et al. [1995], and using Oligo3 and Oligo4 for screening: *MAK3-3* × *MYC*, Oligo24 and Oligo27; *NAT3-3* × *MYC*, Oligo28 and Oligo31; and NAT5-3 × *MYC*, Oligo32, and Oligo33. All TAP- and myc-tagged strains were probed for corresponding protein expression with peroxidase-anti-peroxidase antibody (PAP, Sigma, St. Louis, MO) or mouse monoclonal anti-*myc* antibody (Neomarkers, Fremont, CA).

Preparation and Fractionation of Polyribosomes

Yeast polyribosomes were fractionated by sucrose density gradient centrifugation essentially as described by Baim et al. [1985]. Briefly, various yeast strains were grown in YPD medium to an optical density of about 1.5 at 600 nm. Cultures were placed on ice for 5 min, harvested by centrifugation at 5,000*g* for 5 min, and washed twice with a solution containing 10 mM Tris-HCl, pH 7.5, 100 mM NaCl and 30 mM $MgCl_2$. $MgCl_2$ was omitted in all solution in experiments when the NAT subunit association with dissociated ribosomal particles were tested. The cells were resuspended in a small volume of the same buffer and homogenized with glass beads by vortexing 10 times for 30 s, with incubation for 30 s intervals on ice. Crude extracts were cleared by centrifugation, first at a low speed of 5,000*g* for 5 min, then at 10,000*g* for 10 min. Subsequently portions of the supernatants corresponding to 90 A_{260} units were layered onto an 11.0 ml, 7–47% linear sucrose gradient containing 50 mM Tris-acetate, pH 7.0, 50 mM NH_4Cl, 1 mM dithiothreitol, and either with or without 30 mM $MgCl_2$. The gradients were centrifuged at 41,000*g* for 2 h at 5°C (SW-41 rotor, Beckman L7 Ultracentrifuge) and 500 μl fractions were collected sequentially from the bottom of the gradient, containing the polyribosomal fractions, to the top of the gradient, containing the cytosolic proteins. The gradients without $MgCl_2$ were ultracentifugated for 3.5 h. Protein levels in the fractions were estimated by measuring A_{254} that also was used to prepare the polyribome fraction profiles.

Analysis of the Polyribosome Fractions and Immunoblotting Procedures

One volume of 2× SDS sample buffer was added to the 15 μl portions of the collected fractions; subsequently the fractions were denatured by boiling for 5 min. The proteins were separated by SDS–PAGE, using 4–20% linear precast gels (Gradipore, Frenchs Forest, Australia) and a running condition of 120 V for 90 min; subsequently the separated proteins were transferred to ECL nitrocellulose (Amersham, Piscataway, NJ) and the membranes were immunoblotted with different antibodies. PAP antibody (1:200 dilution) was used to detect the TAP-tagged NAT catalytic subunits; primary rabbit anti-Rpl3p, a core protein of the 60S subunit (1:2,000) and rabbit anti-Rps3p, a core protein of the 40S subunit (1:2,000) [Vetro and Chang, 2002] were used to detect the large and small ribosomal subunits, respectively; and rabbit anti-glucose-6-phosphate dehydrogenase (G6PDH) antibody (Sigma, 1:4,000) was used to locate the cytoplasmic protein, G6PHD. Also, mouse monoclonal anti-*myc* (1:150) and anti-HA (1:500) antibodies were used to detect Mdm20p tagged proteins. The rabbit polyclonal antibody raised against the yeast native Ard1p, Nat1p, Nat3p, and Nat5p were obtained from Dr. S. Rospert (University of Freiburg, Germany), the rabbit anti-Rps14p and anti-Rpl25p were obtained from Dr. Woolford (Carnegie Mellon University) and Dr. K. Siegers (Max Planck Institute of Biochemistry, Martinsried, Germany), respectively. The appropriate secondary goat anti-rabbit or anti-mouse IgG conjugated horse radish peroxidase (Bio-Rad, Hercules, CA, 1:2,000) and ECL Plus kit (Amersham) were used to visualize the protein positive bands on the membranes.

Purification and Characterization of the Yeast NatA Complex and Rpl35p-TAP Associated Proteins

The NatA protein complex was purified by the TAP method with Ard1p-TAP as a bait [Rigaut et al., 1999]. *ADR1* was fused to the TAP tag by PCR-based tagging, using plasmid pAB2629 (originally designated pBS1479 and obtained from B. Séraphin, EMBL, Heidelberg, Germany) as a template and with Oligo21 and Oligo22 (Table III). Neither of the tags, ProtA and CBP, impaired protein function as the *ARD1-TAP* strain grew similarly to the normal strain on different media. The TAP procedure was modified in order to allow the samples to be treated with 20 μg/ml of ribonuclease A (Sigma) for 15 min before protein binding to IgG beads in

order to strip RNA from polyribosomes, resulting in their complete disassembly. Also 5 mM EDTA was added to bind any residual amount of magnesium that promotes subunits assembly. After TEV protease (tobacco etch virus protease) cleavage, the eluted complex was vacuum concentrated, the subunits were separated by electrophoresis in a 4–20% gradient Tris-glycine SDS–PAGE gel, and the protein bands were visualized by BluePage staining (Fermentas, Vilnius, Lithuania).

Rpl35p-TAP and associated proteins were purified by the similar TAP procedure as described above. IgG-bound samples were directly tested by Western blot by probing with various antibodies.

In-Gel Tryptic Digests and Peptide MS Analysis

The protein bands were stained, excised from the gel, washed, reduced, alkylated and then incubated with trypsin essentially as described by Polevoda et al. [2003]. The peptides were desalted using C18 ZipTip (Millipore, Bedford, MA), followed by elution from the tip with 10 μl 50% acetonitrile; immediately prior to injection, the acetonitrile was removed with a Speed-vacuum concentrator and the volume brought to about 2 μl; mass spectrometric (MS) analysis was performed with a Voyager-DE STR linear time-of-flight mass spectrometer (PE Biosystems, Framingham, MA) at the MicroChemical Protein/Peptide Core Facility (University of Rochester). Proteins were identified by searching a comprehensive non-redundant yeast protein database using the program MS-Fit/Prospector (University of California at San Francisco, http://prospector.ucsf.edu/ucsfhtml4.0/msfit.htm). Ribosomal protein peptides were analyzed with a Q-Tof hybrid quadrupole/time-of-flight MS using a nanoelectrospray source (Mass Spectrometry facility, Columbia University). The latter was performed as follows: a fused-silica tip mounting adapter from New Objective (Woburn, MA) was fitted with a 75 μm ID fused silica tip (New Objective), connected through 50 μm ID fused silica tubing to the 1c detector outlet. Nano-LC was performed using LC Packings C18 PepMap 5 μm column with 75 μm ID, 15 cm length, with a flow rate of 200 nl/min, with a 2–80% acetonitrile gradient in 0.1% formic acid and with an ultimate detector having a 10 nl flow cell, and at 214 nm. The processed files were submitted to MASCOT search at http://www.matrixscience.com.

RESULTS

All Yeast NATs Colocalize With Mono- and Polyribosomes

By using chemical peptide crosslinking, Gautschi et al. [2003] previously showed that NatA is quantitatively bound to ribosomes with Nat1p serving as an anchor for the catalytic subunits Ard1p and Nat5p. We applied another procedure, the polyribosome fractionation in a linear sucrose density gradient, to determine whether all major NATs are associated with translating polyribosomes. We investigated NAT subunits localization in the normal strains and in the following series of strains containing the epitope tagged catalytic subunits: *ARD1-TAP*; *NAT3-TAP*; *NAT5-TAP*; *MAK3-TAP*; *MDM20-TAP*; *NAT3-3 × MYC*; and *MAK3-3 × MYC*. In addition, we also investigated a series of mutant strains with deletions of the corresponding auxiliary subunits (Table II). It should be noted that all tagged proteins were functional as the corresponding strains grew normally on the media that we used previously to characterize the appropriate deletion mutants. For example, the *NAT3-TAP* strain, B-13396, was not temperature sensitive (t.s.) or salt sensitive as compared to the *nat3*-Δ mutant [Polevoda et al., 2003]. However, it was not possible to test the *NAT5* fusion strain for proper function as the *nat5*-Δ mutant has no obvious phenotype.

We fractionated the cell extracts in sucrose gradients by a procedure that is commonly used for polyribosome fractionation [Baim et al., 1985]. The fractions from sucrose gradients were loaded on 4–20% gradient SDS–PAGE, the separated proteins were transferred onto ECL nitrocellulose membrane and probed with various antibodies. The α-Rpl3p, anti-ribosomal protein L3, and the α-Rps3p, anti-ribosomal protein S3, antibodies were used to localize polyribosomal fractions as well as ribosomal subunit fractions; α-G6PDH (glucose-6-phosphate dehydrogenase, also designated Zwf1p) antibody was used to detect G6PHD, a negative control for localization of free cytoplasmic proteins.

The results of the experiments, presented in Figure 1, showed that the major portions of the

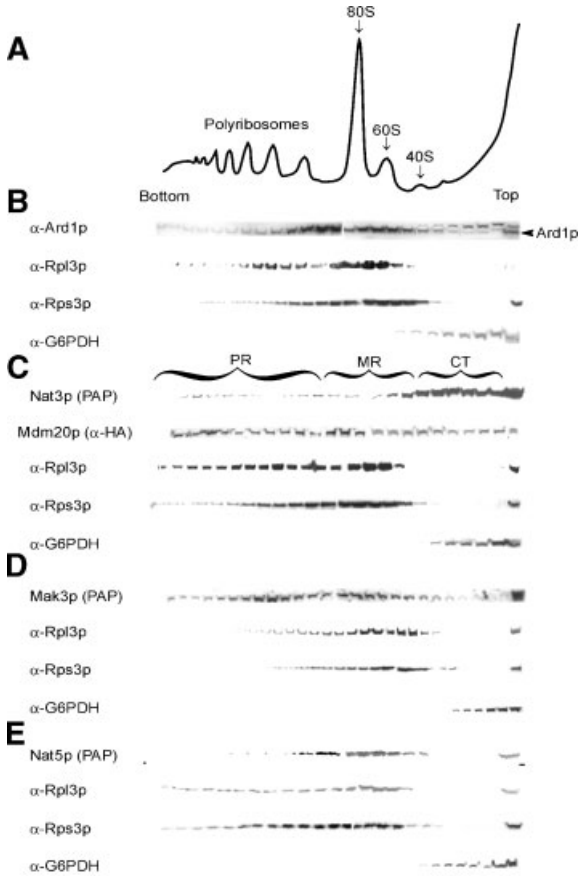

Fig. 1. All tested NAT subunits colocalize with mono- and polyribosomes. **A**: A typical protein absorbance profile of the sucrose gradient, determined spectrophotometrically at 254 nm, is presented for fractions prepared from the normal strain, B-11679; the positions of polyribosomes, and 80S, 60S, and 40S ribosomes are presented. Western blot analysis of the polyribosome fractions prepared from the following yeast strains: (**B**) B-11679, the normal strain; an arrow indicates a position of Ard1p as in cytosolic fractions α-Ard1p recognizes an additional nonspecific band of slightly higher molecular mass; (**C**) B-15511, the normal yeast strain containing *NAT3-TAP* and *MDM20-3 × HA* tagged genes; PR, MR, and CT denote the polyrobosomal, monoribosomal, and cytosolic fractions that were pooled and used in similar experiment with *MDM20-TAP* strain, B-15971, to show copurification of Mdm20p-TAP and Nat3p; (**D**) B-15349, the normal yeast strain containing *MAK3-TAP*; and (**E**) B-15332, the normal yeast strain containing *NAT5-TAP*. The following antibodies were used for Western blot analysis: α-Ard1p, antibody raised against native Ard1p protein; α-Rpl3p, anti-ribosomal protein L3 antibody; α-Rps3p, anti-ribosomal protein S3 antibody; α-G6PDH, anti-glucose-6-phosphate dehydrogenase antibody, used to determine the location of free cytoplasmic proteins; PAP, peroxidase-anti-peroxidase complex for detection of the TAP tagged proteins Nat3p, Nat5p, and Mak3p; and α-HA, HA epitope antibody used for detection Mdm20p-3 × HA. Fractions are shown from the bottom (left) to the top (right) of 7–47% linear sucrose gradients. The results with total cell extracts, serving as positive controls, are shown in the last lane on the right.

NAT subunits, Ard1p (NatA), Mdm20-3 × HA (NatB), Mak3p-TAP (NatC) and Nat5p-TAP (NatE) colocalized to the positions of the ribosomal proteins Rpl3p and Rps3p and with mono- and polyribosome fractions, which corresponded to the bottom part of the sucrose density gradient. On the other hand, a known cytosolic protein, G6PDH, was found only at the top of the gradient. Similar results were obtained with polyribosome fractions prepared from the strains containing MYC tagged Nat3p and Nat5p; TAP tagged Ard1p, Mdm20p, and Mak10p, and also by using the normal strains and antibodies raised against the native proteins, Nat1p, Nat5p, and Nat3p (data not shown). However, in contrast to Mdm20p-3 × HA, a major portion of Nat3p-TAP localized in the top portion of the gradient and only minor amount was associated with polyribosomes (Fig. 1C). It should be noted that we previously showed that Nat3p-TAP and Mdm20p form a complex and that this complex can be purified by the TAP procedure [Polevoda et al., 2003]. Also, a larger portion of Nat5p-TAP localized to the monoribosomal fractions than to the polyribosomal fractions.

We determined whether Nat3p and Mdm20p are associated with each other in different fractions of the gradient by fractionating the cell extract of the *MDM20-TAP* strain, B-15791, and by identifying the polysome (PR), monoribosome (MR), and cytosolic (CT) fractions with α-Rpl3p, α-Rps3p and α-G6PHD antibodies. These PR, MR, and CT fractions (similarly as shown on Fig. 1C) were pooled and Mdm20p-TAP was purified by using standard IgG-Sepharose affinity chromatorgaphy. Proportional amounts of IgG-bound material were loaded onto a 4–20% gradient SDS–PAGE, the separated proteins were transferred onto ECL membrane and probed with various antibodies, including PAP for Mdm20p detection and with α-Nat3p (Fig. 2). The results clearly showed that Mdmd20p and Nat3p are physically associated in these three pooled PR, MR, and CT fractions. Thus, all NATs, including catalytic subunits Ard1p, Nat3p, Mak3p and Nat5p colocalize with mono- and polyribosome fractions, although the majority of Nat3p is located at the top of the gradient, the position of free cytoplasmic proteins. Also, Nat4p-TAP (NatD) was detected primarily in mono- and polyribosome fractions [B. Polevoda, J. Hoskins and F. Sherman, unpublished].

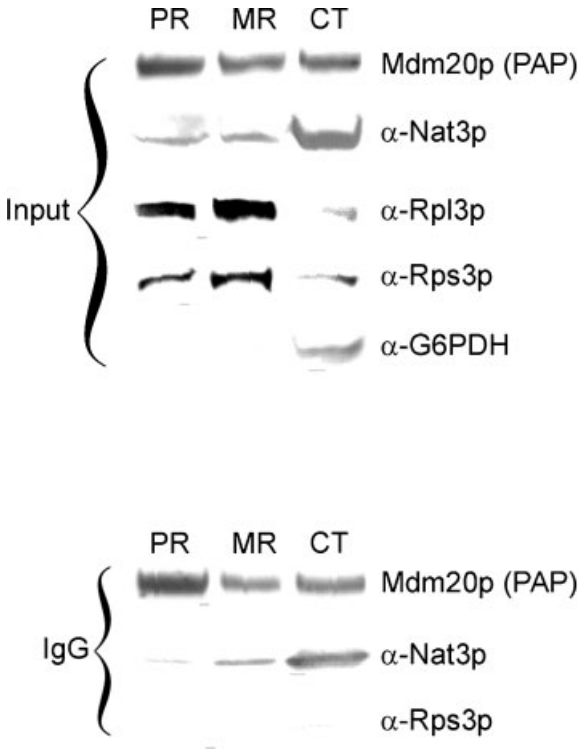

Fig. 2. Mdm20p and Nat3p copurified from polyribosomal fractions. Cell extract of the strain, B-15791, containing *MDM20-TAP*, was fractionated in a 7–47% linear sucrose gradient and the polyribosome (PR), monoribosome (MR), and cytosolic (CT) fractions were detected with α-Rpl3p, α-Rps3p, and α-G6PHD antibodies. Fractions were pooled as shown on Figure 1C and Mdm20p-TAP was purified using IgG-Sepharose affinity chromatorgaphy. IgG-bound proteins were loaded onto 4–20% gradient SDS–PAGE, the separated proteins were transferred onto ECL nitrocellulose membrane and the membrane was probed with PAP antibody to detect Mdm20p, with α-Nat3p to detect Nat3p and with control α-Rpl3p, α-Rps3p, and α-G6PHD (G6PDH) antibodies. Mdm20p-TAP and Nat3p copurified from all three pooled fractions.

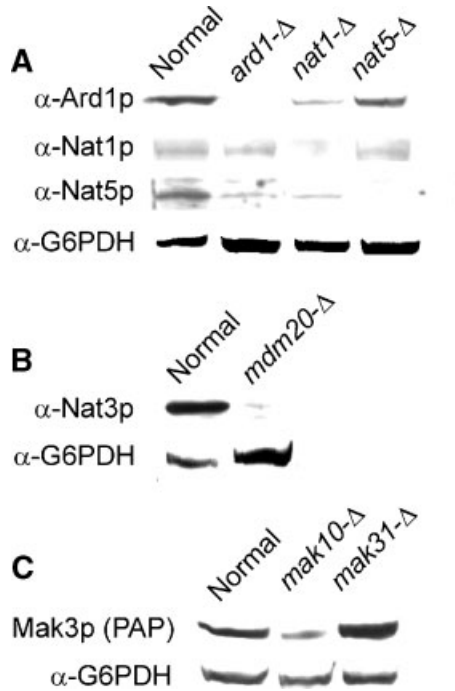

Fig. 3. Stability of the NAT subunits in the deletion mutants. Western blot analysis of the cell extracts from the following yeast strains were carried out: (**A**) Normal (B-11679); *ard1*-Δ (B-11706); *nat1*-Δ (B-11815); *nat5*-Δ (B-13924); (**B**) Normal (B-13396, a normal strain containing *NAT3-TAP*); *mdm20*-Δ (B-15398, a *mdm20*-Δ strain containing *NAT3-TAP*); (**C**) Normal (B-15349, a normal strain containing *MAK3-TAP*); *mak10*-Δ (B-15366, a *mak10*-Δ containing *MAK3-TAP*); *mak31*-Δ (a *mak31*-Δ strain containing *MAK3-TAP*). Equal amounts of about 25 μg of total protein was loaded onto 4–20% gradient SDS–PAGE gels. The levels of G6PDH served as a loading control. Antibodies used are the same as presented in Figure 1.

Deletion of the NAT Auxiliary Subunits Causes Instability of the Corresponding Catalytic Subunit

Gautschi et al. [2003] previously determined that the level of Ard1p bound to the ribosome was diminished in the *nat1*-Δ mutant. We analyzed cell extracts of the following strains to determine the stability of the different NAT subunits in various deletion mutants: the normal strain, B-11679; the *nat1*-Δ mutant, B-11815; the *ard1*-Δ mutant, B-11706; and the *nat5*-Δ mutant, B-13924. Equal amounts of total protein prepared from those strains was loaded onto 4–20% gradient SDS–PAGE, the separated proteins were transferred to ECL membrane and probed with appropriate antibodies (Fig. 3). The results of the Western blots showed that the deletion of *NAT1* caused a significant decrease in the amounts of Ard1p and Nat5p in the cell extracts (Fig. 3A). Also, the deletion of either *ARD1* or *NAT5* caused the diminished levels of the other catalytic subunit, Nat5p or Ard1p, respectively. On the other hand, the deletion of any of *ARD1* or *NAT5* showed much less effect on the levels of Nat1p.

More over, a deletion of the NatB auxiliary subunit gene, *MDM20*, resulted in the most dramatic effect on Nat3p stability; Nat3p was barely detectable in the *mdm20*-Δ cell extract (Fig. 3B). This is rather surprising since a major portion of Nat3p was found in the cytoplasm unassociated with polyribosomes (Fig. 1C), where relatively smaller amount of Mdm20p was detected.

Deletion of NatC auxiliary subunit gene, *MAK10*, caused very similar effect on Mak3p-TAP stability as compared to *NAT1* deletion in

case of NatA (Fig. 3C). This result could be indirect evidence that Mak10p may play a role in attaching NatC to the ribosome, similar to Nat1p. However, *MAK31* deletion caused very little if any effect on Mak3p.

Deletion of the Auxiliary Subunit Nat1p (NatA) but not Mak10p (NatC), Causes Dissociation of the Corresponding Catalytic Subunit From Polyribosomes

Cell extracts from the normal strain, B-11679, and the *nat1*-Δ mutant, B-11815, were fractionated and the effect of the NAT auxiliary subunit deletion on the catalytic subunit localization in sucrose gradient was determined. In addition to the significantly lower levels of Ard1p in the *nat1*-Δ mutant sample, we clearly observed an altered Ard1p localization with only minor amounts in the fractions containing both Rpl3p and Rps3p (Fig. 4A) as compared to the sample from the normal strain (Fig. 1B). In contrast, in similar experiments with *mak10*-Δ cell extract containing Mak3p-TAP, we did not observe a significant change in Mak3p-TAP

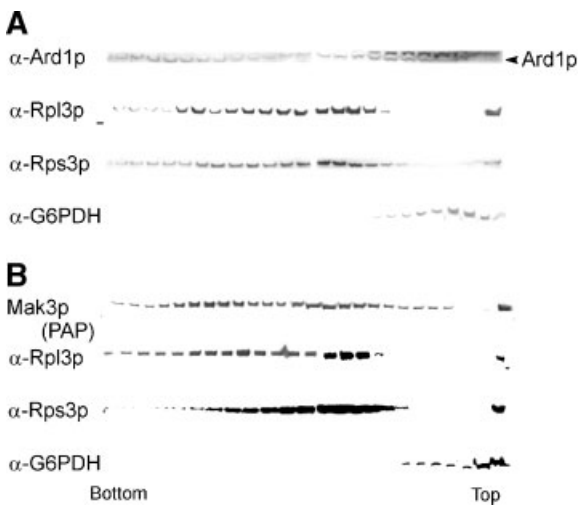

Fig. 4. The effect of deletions on the levels and distribution of NAT subunits. Western blot analysis was carried out with the 7–47% linear sucrose gradient fractions prepared from the following strains: (**A**) B-11815, *nat1*-Δ deletion strain; a nonspecific band, which responds to α-Ard1p, but which has a slightly higher molecular mass than Ard1p, is indicated with an arrow; and (**B**) B-15366, *mak10*-Δ deletion strain containing *MAK3-TAP* tagged gene. Ard1p localization is altered in the *nat1*-Δ strain with a major portion of the protein in the cytoplasm as compared to the normal strain, B-11679 (Fig. 1B). Only traces of Ard1p were present in the fractions containing both Rpl3p and Rps3p. In contrast, Mak3p-TAP localization did not changed significantly in *mak10*-Δ cells as compared to the normal strain, B-15349 (Fig. 1D). Antibodies used are the same as presented in Figure 1.

localization (Fig. 4B) as compared to the normal strain (Fig. 1D). Moreover, the deletion of *mak31*-Δ or double *mak10*-Δ *mak31*-Δ deletions did not significantly alter the Mak3p-TAP protein localization in sucrose gradient (data not shown). This may indicate that the Mak3p itself can bind to the ribosome, although it is not excluded that the TAP tag affects Mak3p-TAP localization. (It would be desirable to use in such experiments α-Mak3p, an antibody raised against the native protein, but this antibody is not available). It is noteworthy that AtMAK3, an *Arabidopsis thaliana* Mak3p protein ortholog, can functionally replace the yeast Mak3p alone in acetylating of the N termini of endogenous proteins and the L-A virus Gag protein, even when *mak10*-Δ and *mak31*-Δ are deleted in combination with *mak3*-Δ [Pesaresi et al., 2003]. This result, together with the finding that knock-out of the *Arabidopsis MAK10* homolog did not result in obvious physiological effects in plants, indicate that *AtMAK3* function may not require NatC complex formation for efficient N-terminal acetylation, as it does in yeast.

Also, it was not possible to investigate how the *mdm20*-Δ deletion affects Nat3p localization in sucrose gradient because the corresponding strain contained only barely detectable levels of Nat3p (see the section above and Fig. 3B).

NAT Subunits Still Colocalize With Dissociated Ribosomal Subparticles

Subsequently, we investigated the association of NAT subunits with monoribosomes and monoribosomal subparticles generated by dissociation of polyribosomes by the lack of Mg^{++}. A cell extract of the normal strain, B-11679, was prepared using a buffer lacking Mg^{++}, the extract was fractionated in a sucrose density gradient without Mg^{++} (Fig. 5A,B), and the positions of the ribosomal proteins were determined with Rpl3p and Rps3p antibodies. Under these conditions, the polyribosomes were disrupted, although the 80S did not completely dissociated into 60S and 40S, and the ribosomal proteins were clearly absent from the bottom portion of the gradient (Fig. 1B). Ard1p colocalized with both Rpl3p and Rps3p containing fractions and was not shifted to the top of the gradient, corresponding to the free cytoplasmic fractions. In similar experiments, we found that Mak3p-TAP (strain B-15349) remained associated with monoribosomes when the

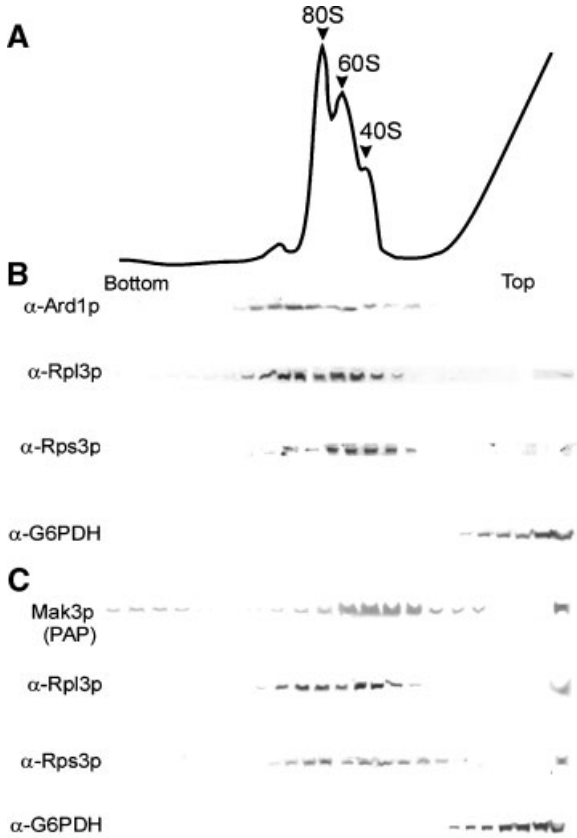

Fig. 5. NAT subunits are still associated with monoribosomal subparticles when polyribosomes are dissembled. **A**: A typical protein absorbance profile of the sucrose gradient, lacking magnesium, is presented for fractions prepared from the normal strain. Polyribosomes were completely disrupted; however 80S monoribosomes did not completely dissociate into 60S and 40S. **B**,**C**: Western blot analysis of the 7–47% linear sucrose gradient fractions prepared without magnesium in the buffer from: (B) B-11679, the normal strain; and (C) B-15349, the normal strain containing *MAK3-TAP*. Although polyribosomes are no longer detectable in the lower portion of the gradient, Ard1p and Mak3p-TAP proteins colocalized with both Rpl3p and Rps3p. Antibodies used are the same as presented in Figure 1.

corresponding strain cell extract was fractionated using a buffer lacking Mg^{++} (Fig. 5C), while Nat3p-TAP (strain B-13396) remained at the top of the gradient (results not shown). It should be noted that the protein levels of all three NAT catalytic subunits were clearly reduced (Fig. 5) in the gradients without Mg^{++} as compared to the Mg^{++}-containing gradients (Fig. 1).

Identification of the Specific Ribosomal Proteins Associated With NatA

Potential ribosome attachment sites to the NATs were identified with most characterized NAT, NatA, and by using the TAP procedure that provides the advantage of using strains with normal physiological levels of protein expression [Rigaut et al., 1999]. The *ARD1-TAP* fusion gene was constructed by the PCR-based tagging procedure and the resulted yeast strain, B-14260 (Table II), grew normally on YPD and YPG at 37°C, in contrast to *ard1*-Δ or *nat1*-Δ mutants, which exhibited t.s. phenotypes [Mullen et al., 1989]. The expression of the Ard1p fusion protein in strain B-14260 was verified by Western blot analysis and the presence of a positive band of 41 kDa, indicating that the molecular mass of Ard1p-TAP corresponded to the expected value (data not shown). Cell extract of the normal strain, B-10190, lacking a TAP tag, served as a negative control in purification experiments and showed no specific bands except IgG contaminants and TEV bands (Fig. 6A).

The Ard1p fusion and associated proteins were recovered by TAP affinity chromatography on IgG-agarose beads. The TEV cleaved complex was concentrated, the components were separated by SDS–PAGE, and the protein bands were visualized by Coomassie staining (Fig. 6A). The proteins were identified by standard peptide matching techniques: bands were excised from a gel, washed, reduced, alkylated, and digested with trypsin, the resulting peptides were analyzed by MALDI-TOF MS, and peptide masses were compared to the known yeast proteins. In addition to the two major contaminants of IgG heavy and light chains immunoglobulins, which were used for affinity to bind TAP tagged proteins, and which were seen as about 45 and 25 kDa bands, respectively, several other proteins were clearly observed on a gel with the following molecular masses: 100 kDa; 41 kDa; double band around 30 kDa and two low molecular mass bands. The 30 kDa bands were very characteristic and appeared to correspond to TEV protease. The 100 kDa band from NatA complex was identified as Nat1p, as several peptides covering over 40% of the primary amino acid sequence had the expected molecular masses (data not shown). Similarly, the 41 kDa band was found to correspond to Ard1p-CBP protein (data not shown). Nat5p protein band was not well separated on the gel and its position was masked by a much higher intensity band of the IgG light chain of about 25 kDa, although it was detected by Western

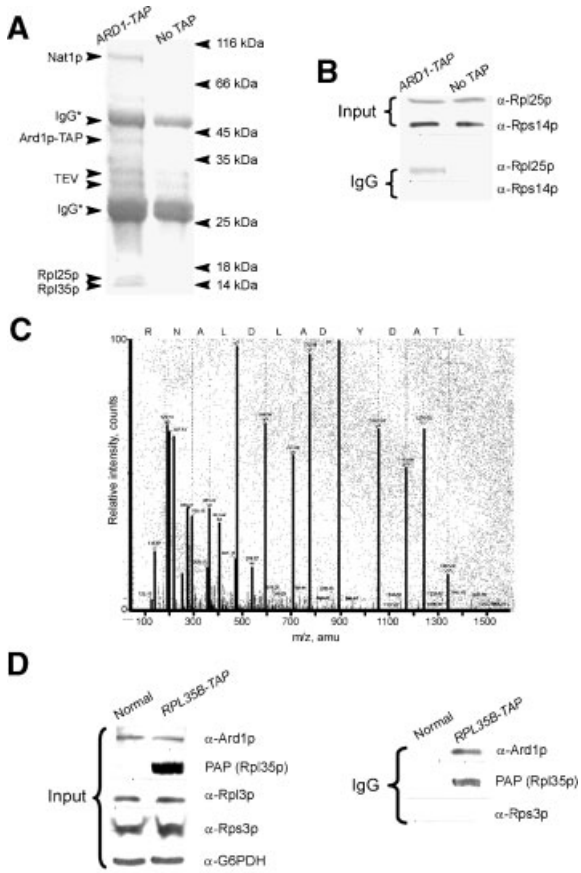

Fig. 6. Ribosomal proteins Rpl25p and Rpl35p copurify with NatA. **A**: IgG affinity purified samples from the *ARD1-TAP* strain and the normal (no TAP) strain after the TEV protease cleavage were loaded onto 4–20% gradient SDS–PAGE and the separated proteins were identified by mass spectrometry. Positions of Ard1p-TAP, Nat1p, Rpl25p, and Rpl35p are indicated on the left of the gel, as are the positions of IgG heavy and light chain contaminants (IgG*) and two TEV protease bands (TEV). Molecular mass markers are on the right side of the figure. **B**: Rpl25p copurifies with Ard1p-TAP. IgG purified samples from the *ARD1-TAP* and the normal strains were probed with α-Rpl25p and α-Rps14p antibodies. Only *ARD1-TAP* sample showed a positive Rpl25p-specific signal. **C**: MS–MS spectrum and the sequence of the Rpl25p specific peptide detected in the Ard1p-CBP sample. **D**: Ard1p copurifies with Rpl35p-TAP. Cell extracts from the normal strain, B-14276, and from the corresponding *RPL35B-TAP* strain, B-15925, were subjected to IgG-Sepharose affinity chromatography. IgG-bound proteins were loaded onto 4–20% gradient SDS–PAGE, the separated proteins were transferred onto ECL membrane and the membrane was probed with PAP antibody to detect Rpl35p-TAPp, with α-Ard1p to detect Ard1p and with control α-Rpl3p, α-Rps3p and α-G6PDH antibodies. In contrast to the sample from the normal strain, IgG-purified sample from *RPL35B-TAP* strain contained Ard1p.

blot and probing with α-Nat5p antibody (data not shown).

In addition to the NatA subunits, we were interested in other associated proteins, primarily ribosomal proteins, which mainly have the molecular masses from 10 to 25 kDa, and which are usually located in the lower portion of the gel. Two protein bands seen over background were observed in this region of the gel (Fig. 6A). Although tryptic peptides of the corresponding proteins matched to several candidate ribosomal proteins, the background on MS spectra was relatively high. Therefore, we used Q-Tof hybrid quadrupole/time-of-flight MS with a nanoelectrospray source that allowed us to obtain the sequences of the tryptic peptides. The RP bands of the gel were excised, treated as above and the resulting peptides were analyzed by Q-Tof MS. Based on the molecular masses and peptide sequences, the two ribosomal proteins were identified: (a) Rpl25p, with predicted protein molecular mass 15.6 kDa and the sequenced peptide, LTADYDALDIANR, (Fig. 6B); and (b) Rpl35p, 13.9 kDa, SIACVLTVINEQQR (MS data not shown). Thus, these ribosomal proteins may play a role in the attachment of NatA to the ribosome. At least, both Rpl25p and Rpl35p were described as located in close proximity to the ribosomal polypeptide exit [Morgan et al., 2002; Grallath et al., 2006].

Additional evidence for association of NatA with those ribosomal proteins were obtained by carrying out the following experiments. First, we tested Ard1p-TAP sample for the presence of Rpl25p by probing with anti-Rpl25p antibody. The results clearly showed that Rpl25p copurified with Ard1p-TAP (Fig. 6B), while the control protein Rps14p did not. Second, we used *RPL35B-TAP* tagged strain, B-15925, and the normal *RPL35B* strain, B-14276, as a negative control, to purify Rpl35p-TAP and to examine whether it was associated with Ard1p. Rpl35p-TAP was purified similarly to Ard1p-TAP, with extensive RNAse A treatment and with addition of EDTA to remove any residual amount of Mg^{++} and to completely dissemble the ribosome structure. The resulting protein samples were probed with PAP (for Rpl35p-TAP) and α-Ard1p antibodies (Fig. 6D). Clearly, Ard1p copurified with Rpl35p-TAP while no Ard1p was detected in the sample prepared from the normal strain. We also tested both IgG purified samples for the presence of another ribosomal protein Rps3p, a small subunit protein; however no detectable signal was obtain in any of these samples (Fig. 6D).

DISCUSSION

All NATs are Associated With Mono- and Polyribosome

In this study we used polyribosome fractionation in a linear sucrose density gradient to establish that all major NATs, NatA, NatB, NatC, and NatE, are associated with ribosomes (Table IV). The major portions of the catalytic subunits Ard1p, Mak3p, and Nat5p, and the auxiliary subunits Nat1p, Mdm20p, and Mak10p all colocalize with mono- and polyribosome fractions (Fig. 1). However, the bulk of Nat3p is found in the free cytoplasmic fraction and only a minor portion of Nat3p is associated with polyribosome (Fig. 1). The auxiliary subunits Nat1p and probably Mdm20p may serve as NAT anchors providing a stable binding of the catalytic subunits to the ribosome, although it is not excluded that at least Mak3p and possibly Ard1p have an affinity to the ribosome by themselves. Consistent with this view, we observed that in *nat1*-Δ mutant, Ard1p localization is altered in the gradient with only traces of the proteins in fractions containing both ribosomal proteins Rpl3p and Rps3p (Fig. 4). Moreover, as we previously demonstrated, the deletions of the *NAT1*, *MAK10*, and *MDM20* caused the lack of acetylation of the corresponding substrates [Polevoda et al., 1999, 2003; Polevoda and Sherman, 2001]. Thus, NAT subunit interactions is not only required for biochemical activity but it is also possible that attachment to the ribosome is essential for their function. In addition, the auxiliary subunits may be responsible for efficient protein substrate recognition and binding, and for NAT positioning around the ribosome exit tunnel. Acetylated N-terminal sequences, even of the same type, are highly degenerate, especially NatA substrates [Jörnvall 1975; Lee et al., 1989] and the recognition of diversed substrates may require more complex machinery than just one catalytic subunit.

All three auxillary subunits, Nat1p, Mdm20p, and Mak10p contain at least five to seven tritetracopeptide repeats (TPR), which have been found in a variety of proteins, including chaperones and proteins involved in protein transport, and which, as we suggested previously [Polevoda and Sherman, 2003b], may be involved in binding to the ribosome and/or newly synthesized polypeptides. In addition, the deletions of *NAT1*, *MAK10*, and especially *MDM20*, caused significantly decreased the protein levels of the corresponding catalytic subunits Ard1p, Mak3p, and Nat3p, respectively (Fig. 3). However, *MAK31* deletion caused very little, if any, effect on Mak3p stability and the role of Mak31p in N-terminal acetylation is still unclear. Also we observed that the *ard1*-Δ deletion affects the Nat5p level and that the *nat5*-Δ deletion affects the Ard1p level, while Nat1p stability in *ard1* and *nat5* mutants was not significantly affected.

Nat3p has Two Functions?

In spite of the fact that both Nat3p and the auxiliary subunit Mdm20p are required for NatB type acetylation, that both copurify with

TABLE IV. Constitutions of Strains That Have Been Examined for Subunit Association With Polyribosomes

Subunit	Deleted genes	Ref.
Ard1p	None	a,b
	nat1-Δ	a,b
Nat1p	None	a,b
	ard1-Δ	a,b
Nat3p	None	b,c
	mdm20-Δ	b
Mdm20p	None	b
	nat3-Δ	b
Mak3p	None	b
	mak10-Δ	b
	mak31-Δ	b
	mak10-Δ *mak31*-Δ	b
Mak10p	None	b
Mak31p	None	e
Nat4p	None	d
Nat5p	None	a,b
	nat1-Δ	a,b
	ard1-Δ	a,b

a, Gautschi et al. [2003]; b, this work; c, S. Rospert, unpublished; d, Polevoda and Sherman, unpublished; e, not determined.

each other, and that mutants with deletions of either Nat3p or Mdm20p have similar growth phenotypes [Polevoda et al., 2003], it is of importance to note that a greater portion of Nat3p is located in the cytoplasmic fraction than with the ribosomes. In addition to the difference in cellular localization, *nat3*-Δ and *mdm20*-Δ mutants each showed slight variation in distribution of the tropomyosin and in vacuole staining in the cell, with the *mdm20* mutant having a more severe defect [Singer and Shaw, 2003]. Also, Caesar et al. [2006] observed slight differences in the quantitative growth of the *nat3*-Δ and *mdm20*-Δ strains in synthetic liquid media containing various inhibitors. These findings lead us to suggest that Nat3p has two modes of action. In addition to serving as the catalytic subunit in the Nat3p-Mdm20p-ribosome complex, Nat3p may act by itself either to augment the acetylation NatB substrates, or to acetylate a different class of proteins. Identifying a substrate acetylated by Nat3p alone clearly would be of interest. Also it has not been excluded that the NatB complex is more dynamic than other NAT complexes or that the gene expression level of *MDM20* is different from *NAT3* expression.

NATs are Still Associated With Monoribosomal Subparticles When Polyribosomes are Dissembled

Similar to NAT subunits localization, another N-terminal processing protein, Map1p, that acts upstream of NATs in N-terminal protein processing, was found associated with ribosomes [Vetro and Chang, 2002]. In the presence of magnesium, Map1p was detected throughout the sucrose gradient in the cytosolic, 40S subunit, 60S subunit, and 80S translational complex fractions. In the absence of Mg^{++} magnesium the majority of wild-type Map1p was detected in the 60S subunit fractions containing Rpl3p. Also, lower levels of Map1p were observed in the 40S subunit fractions that did not closely reflected the levels of a core 40S protein Rps3p.

In our experiments, we also found that Ard1p (NatA) and Mak3p (NatC) proteins remained associated with ribosomal subparticles (Fig. 5), when the corresponding strain cell extracts were fractionated in sucrose gradient using a buffer without Mg^{++}. It appears that NATs in this respect are similar to MAPs, colocalizing with fractions containing both Rpl3p and Rps3p. Although a longer sucrose gradient or an alternative approach is required to more precisely localize the NAT proteins to the large or small ribosomal subunit, it is important to stress that both catalytic proteins, Ard1p and Mak3p, colocalized with ribosomal subunits and were not detected in the free cytoplasm when polyribosomes were disrupted, suggesting that they are all ribosome-associated even in an inactive form. Also, although these NAT catalytic subunits were detected at the lower levels in gradients lacking Mg^{++}, as compared to their levels in gradients containing Mg^{++}, the levels of catalytic subunits were significantly higher than their levels in gradients from auxiliary subunit deletion mutants, indicating that polysome disassociation did not cause a rapid degradation.

NatA is Possibly Attached to the Ribosome at the Ribosomal Exit Tunnel

We uncovered two ribosomal proteins in the NatA sample that was biochemically purified using TAP affinity chromatography at the parameters when the polyribosomes were dissembled to subparticles (Fig. 6). Based on the peptide molecular masses and their primary sequences, these ribosomal proteins physically associated with NatA were identified as Rpl25p and Rpl35p. Both Rpl25p and Rpl35p are located very close to the ribosomal exit tunnel [Morgan et al., 2002; Wegrzyn and Deuerling, 2005; Grallath et al., 2006]. Moreover, we obtained additional evidence for the possible physical association of Ard1p and Rpl35p in Rpl35p-TAP copurification experiment and of Ard1p and Rpl25p by directly probing the Ard1p-TAP sample with α-Rpl25p (Fig. 6B,D). Although various RPs are often contaminate TAP-purified complexes, Rpl25p and Rpl35p were detected in Ard1p-TAP sample in a range of equimolar amounts with NatA subunits (Fig. 6A).

In yeast, two protein complexes, NAC and the Hsp70 homologues, Ssb1p and Ssb2p, were shown to bind close to the ribosome exit tunnel and interact with a variety of nascent polypeptides [Rassow and Pfanner, 1996; Gautschi et al., 2001, 2002; Rospert et al., 2002], in addition to Nat1p. A direct comparison revealed that Nat1p required longer nascent polypeptides for interaction than NAC and Ssb1p/Ssb2p [Gautschi et al., 2003]. Nat1p only formed a cross-link to Mdh1p substrate longer than 100 amino acids, or 86 residues for Rpl4A and 87 for

pre-pro α-peptides, while yeast NAC interacts with nascent chains of 72 and 86 amino acids long [Reimann et al., 1999]. Thus, Nat1p binding requires longer nascent chains than cross-link formation with either NAC or Ssb1p/Ssb2p. Obviously NatA acts on newly synthesized polypeptides downstream of NAC and Ssb1p/Ssb2p.

Interestingly, it was reported that the yeast NAC and the signal-recognition particle (SRP) share the universally conserved ribosomal protein Rpl25p as a docking site on the ribosome [Kramer et al., 2002; Pool et al., 2002; Wegrzyn and Deuerling; 2005; Grallath et al., 2006]. In addition, the NAC α-subunit was found to interact with the 54 kDa subunit of SRP. These results, together with our finding of possible Rpl25p association with NatA, identify Rpl25p as a conserved interaction platform for specific cytosolic factors that guide nascent polypeptides to their proper N-terminal processing and cellular destination. On the other hand, we observed colocalization of the NatC catalytic subunit, Mak3p, preferentially with Rps3p-containing fractions in sucrose gradients with disrupted polyribosomes (Fig. 5). Experiments with Map1p also indicated its association with both 60S and 40S ribosome subunits, although there was lower affinity to the 40S subunit [Vetro and Chang, 2002]. The actual mechanism of the MAPs and NATs recruitment to the ribosome remains to be investigated, although it is clear that both are associated with the ribosome even without a proper substrate, that is, when polyribosomes are dissembled (Fig. 5) [Vetro and Chang, 2002; Gautschi et al., 2003].

Because methionine is cleaved before N-terminal acetylation, it would be interesting to determine if MAPs and NATs interact directly and whether they form a larger biochemical complex. Also, it would be of interest to know how MAPs, NATs, NAC, and SRP are organized around the ribosome exit site, which components they share and what is the precise hierarchy of their binding to the ribosome and to an appropriate substrate. It is worthy to note that certain Map^{-}, Nat^{-}, and Nac^{-} mutants grow slower or are t.s. and osmotic sensitive, as are the mutants defective in translation initiation [Uesono and Toh, 2002], protein folding [Rospert et al., 2002] or the mutants lacking certain ribosomal proteins. It remains to be seen if these common defective traits are due to the same deficiency such as the lack of N-terminal acetylation.

ACKNOWLEDGMENTS

We are grateful to Dr. S. Rospert (University of Freiburg) for a gift of the α-Ard1p, α-Nat1p, α-Nat3p, and α-Nat5p antibodies and for many fruitful discussions. We are thankful to Dr. Y-H. Chang (St. Louis University School of Medicine) for the α-Rpl3p and α-Rps3p antibodies, Dr. Woolford (Carnegie Mellon University) for the rabbit α-Rps14p, Dr. K. Siegers (Max Planck Institute of Biochemistry, Martinsried, Germany) for the α-Rpl25p and Dr. B. Séraphin (EMBL, Heidelberg, Germany) for plasmid pBS1479. We greatly appreciate Fan Xia and Jason Hoskins for their contributions to the certain experiments at the initial stage of this study. Special thanks to M.-A. Gawinowicz (Columbia University) for excellent help in protein identification by mass spectrometry and Dr. G. Bedi (MicroChemical Protein/Peptide Core Facility, University of Rochester).

REFERENCES

Baim SB, Pietras DF, Eustice DC, Sherman F. 1985. A mutation allowing an mRNA secondary structure diminishes translation of *Saccharomyces cerevisiae* iso-1-cytochrome *c*. Mol Cell Biol 5:1839–1846.

Caesar R, Warringer J, Blomberg A. 2006. Physiological importance and identification of novel targets for the N-terminal acetyltransferase NatB. Eukaryot Cell 5:368–378.

Driessen HPC, de Jong WW, Tesser GI, Bloemendal H. 1985. The mechanism of N-terminal acetylation of proteins. CRC Crit Rev Biochem 18:281–325.

Gautschi M, Lilie H, Fünfschilling U, Mun A, Ross S, Lithgow T, Rücknagel P, Rospert S. 2001. RAC, a stable ribosome-associated complex in yeast formed by the DnaK-DnaJ homologs Ssz1p and zuotin. Proc Natl Acad Sci USA 98:3762–3767.

Gautschi M, Mun A, Ross S, Rospert S. 2002. A functional chaperone triad on the yeast ribosome. Proc Natl Acad Sci USA 99:4209–4214.

Gautschi M, Just S, Mun A, Ross S, Rücknagel P, Dubaquié Y, Ehrenhofer-Murray A, Rospert S. 2003. The yeast N^{α}acetyltransferase NatA is quantitatively anchored to the ribosome and interacts with nascent polypeptides. Mol Cell Biol 23:7403–7414.

Geissenhoner A, Weise C, Ehrenhofer-Murray AE. 2004. Dependence of ORC silencing function on NatA-mediated Nα acetylation in *Saccharomyces cerevisiae*. Mol Cell Biol 24:10300–10312.

Glover CJ, Hartman KD, Felsted RL. 1997. Human N-myristoyltransferase amino-terminal domain involved in targeting the enzyme to the ribosomal subcellular fraction. J Biol Chem 272:28680–28689.

Grallath S, Schwarz JP, Bottcher UM, Bracher A, Hartl FU, Siegers K. 2006. L25 functions as a conserved ribosomal docking site shared by nascent chain-associated complex and signal-recognition particle. EMBO Rep 7:78–84.

Jackson R, Hunter T. 1970. The effect of cobalt on the synthesis of globin and haem in reticulocytes. FEBS Lett 9:61–63.

Jörnvall H. 1975. Acetylation of protein *N*-terminal amino groups: Structural observations on α-amino acetylated proteins. J Theor Biol 55:1–12.

Kecskes E, Sures I, Gallwitz D. 1976. Initiation of synthesis of *N*-terminal acetylated histones with methionine. Biochemistry 15:2541–2546.

Kido H, Vita A, Hannappel E, Horecker BL. 1981. Aminoterminal acetylation of synthetic *N*α-desacetyl thymosin α1. Arch Biochem Biophys 208:95–100.

Kramer G, Rauch T, Rist W, Vorderwulbecke S, Patzelt H, Schulze-Specking A, Ban N, Deuerling E, Bukau B. 2002. L23 protein functions as a chaperone docking site on the ribosome. Nature 419:171–174.

Lee FJ, Lin LW, Smith JA. 1989. *N*α-acetyltransferase deficiency alters protein synthesis in *Saccharomyces cerevisiae*. FEBS Lett 256:139–142.

Malkin LI, Rich A. 1967. Partial resistance of nascent polypeptide chains to proteolytic digestion due to ribosomal shielding. J Mol Biol 26:329–346.

Morgan DG, Menetret JF, Neuhof A, Rapoport TA, Akey CW. 2002. Structure of the mammalian ribosome-channel complex at 17A resolution. J Mol Biol 324:871–886.

Mullen JR, Kayne PS, Moerschell RP, Tsunasawa S, Gribskov M, Colavito-Shepanski M, Grunstein M, Sherman F, Sternglanz R. 1989. Identification and characterization of genes and mutants for an *N*-terminal acetyltransferase from yeast. EMBO J 8:2067–2075.

Palmiter RD, Gagnon J, Walsh KA. 1978. Ovalbumin: A secreted protein without transient hydrophobic leader sequence. Proc Natl Acad Sci USA 75:94–98.

Park EC, Szostak JW. 1992. ARD1 and NAT1 proteins form a complex that has *N*-terminal acetyltransferase activity. EMBO J 11:2087–2093.

Pesaresi P, Gardner N, Masiero A, Dietzmann S, Eichacker A, Wickner R, Salamini F, Leister D. 2003. Cytoplasmic *N*-terminal protein acetylation is required for efficient photosynthesis in Arabidopsis. Plant Cell 15:1817–1832.

Pestana A, Pitot HC. 1974. *N*-terminal acetylation of histone-like nascent peptides on rat liver polyribosomes in vitro. Nature 247:200–202.

Pestana A, Pitot HC. 1975a. Acetylation of ribosome-associated proteins in vitro by an acetyltransferanse bound to rat liver ribosomes. Biochemistry 14:1397–1403.

Pestana A, Pitot HC. 1975b. Acetylation of nascent polypeptide chains on rat liver polyribosomes in vivo and in vitro. Biochemistry 14:1404–1412.

Polevoda B, Sherman F. 2000. *N*α-terminal acetylation of eukaryotic proteins. J Biol Chem 275:36479–36482.

Polevoda B, Sherman F. 2001. NatC N^{α}-terminal acetyltransferase of yeast contains three subunits, Mak3p, Mak10p and Mak31p. J Biol Chem 276:20154–20159.

Polevoda B, Sherman F. 2003a. *N*-terminal acetyltransferases and sequence requirements for N-terminal acetylation of eukaryotic proteins. J Mol Biol 325:595–622.

Polevoda B, Sherman F. 2003b. Composition and function of the eukaryotic N-terminal acetyltransferase subunits. Biochem Biophys Res Commun 308:1–11.

Polevoda B, Norbeck J, Takakura H, Blomberg A, Sherman F. 1999. Identification and specificities of *N*-terminal acetyltransferases from *Saccharomyces cerevisiae*. EMBO J 18:6155–6168.

Polevoda B, Cardillo TS, Doyle TC, Bedi GS, Sherman F. 2003. Nat3p and Mdm20p are required for function of yeast NatB *N*α-terminal acetyltransferase and of actin and tropomyosin. J Biol Chem 278:30686–30697.

Pool MR, Stumm J, Fulga TA, Sinning I, Dobberstein B. 2002. Distinct modes of signal recognition particle interaction with the ribosome. Science 297:1345–1348.

Rassow J, Pfanner N. 1996. Protein biogenesis: Chaperones for nascent polypeptides. Curr Biol 6:115–118.

Reimann B, Bradsher J, Franke J, Hartmann E, Wiedmann M, Prehn S, Wiedmann B. 1999. Initial characterization of the nascent polypeptide-associated complex in yeast. Yeast 15:397–407.

Rich A, Eikenberry EF, Malkin LI. 1966. Experiments on hemoglobin polypeptide chain initiation and on the shielding action of the ribosome. Cold Spring Harb. Symp Quant Biol 31:303–310.

Rigaut G, Shevchenko A, Rutz B, Wilm M, Mann M, Séraphin B. 1999. A generic protein purification method for protein complex characterization and proteome exploration. Nature Biotechnol 17:1030–1032.

Rospert S, Dubaquie Y, Gautschi M. 2002. Nascent-polypeptide-associated complex. Cell Mol Life Sci 59: 1632–1639.

Schneider BL, Seufert W, Steiner B, Yang QH, Futcher AB. 1995. Use of polymerase chain reaction epitope tagging for protein tagging in Saccharomyces cerevisiae. Yeast 11:1265–1274.

Sherman F. 2002. Getting started with yeast. Methods Enzymol 350:3–41.

Singer JM, Shaw JM. 2003. Mdm20 protein functions with Nat3 protein to acetylate Tpm1 protein and regulate tropomyosin-actin interactions in budding yeast. Proc Natl Acad Sci USA 100:7644–7649.

Singer JM, Hermann GI, Shaw JM. 2000. Suppressors of mdm20 in yeast identify new alleles of ACT1 and TPM1 predicted to enhance actin-tropomysin interactions. Genetics 156:523–534.

Song OK, Wang X, Waterborg JH, Sternglanz R. 2003. An N^{α}-acetyltransferase responsible for acetylation of the N-terminal residues of histones H4 and H2A. J Biol Chem 278:38109–38112.

Strous GJ, Berns AJ, Bloemendal H. 1974. *N*-terminal acetylation of the nascent chains of α-crystallin. Biochem Biophys Res Commun 58:876–884.

Tercero JC, Wickner RB. 1992. MAK3 encodes an *N*-acetyltransferase whose modification of the L-A gag NH2 terminus is necessary for virus particle assembly. J Biol Chem 267:20277–20281.

Tercero JC, Dinman JD, Wickner RB. 1993. Specificity of the yeast MAK3 *N*-acetyltransferase that modifies gag of the L-A dsRNA virus. J Bacteriol 175:3192–3194.

Traugh JA, Sharp SB. 1977. Protein modification enzymes associated with the protein-synthesizing complex from rabbit reticulocytes. Protein kinase, phosphoprotein phosphatase, and acetyltransferase. J Biol Chem 252: 3738–3744.

Traugh JA, Sharp SB. 1979. Isolation of acetyltransferase activities from rabbit reticulocytes and modification of translational components. Methods Enzymol 60:534–541.

Tsunasawa S, Sakiyama F. 1984. Amino-terminal acetylation of proteins: An overview. Methods Enzymol 106: 165–170.

Uesono Y, Toh EA. 2002. Transient inhibition of translation initiation by osmotic stress. J Biol Chem 277:13848–13855.

Uetz P, Giot L, Cagney G, Mansfield TA, Judson RS, Knight JR, Lockshon D, Narayan V, Srinivasan M, Pochart P, Qureshi-Emili A, Li Y, Godwin B, Conover D, Kalbfleisch T, Vijayadamodar G, Yang M, Johnston M, Fields S, Rothberg JM. 1999. A comprehensive analysis of protein-protein interactions in *Saccharomyces cerevisiae*. Nature 403:623–627.

Vetro JA, Chang YH. 2002. Yeast methionine aminopeptidase type 1 is ribosome-associated and requires its *N*-terminal zinc finger domain for normal function in vivo. J Cell Biochem 85:678–688.

Wang X, Connelly JJ, Wang CL, Sternglanz R. 2004. Importance of the Sir3 N terminus and its acetylation for yeast transcriptional silencing. Genetics 168:547–551.

Wegrzyn RD, Deuerling E. 2005. Molecular guardians for newborn proteins: Ribosome-associated chaperones and their role in protein folding. Cell Mol Life Sci 62:2727–2738.